



# The Open Fuels & Energy Science Journal

Content list available at: [www.benthamopen.com/TOEFJ/](http://www.benthamopen.com/TOEFJ/)

DOI: 10.2174/1876973X01811010001



## RESEARCH ARTICLE

# The Effect of $\text{CaBr}_2$ on Mercury Speciation in Flue Gas: An Experimental and DFT Study

Jun Zhong<sup>1</sup>, Fangyong Li<sup>1</sup> and Weijie Yang<sup>2,\*</sup><sup>1</sup>Electric Power Science Research Institute of Guangdong Power Grid Co. Ltd., Guangzhou, China<sup>2</sup>School of Energy and Power Engineering, North China Electric Power University, Baoding, China

Received: September 28, 2017

Revised: January 15, 2018

Accepted: January 18, 2018

### Abstract:

#### Background:

Additives affect the formation of different mercury speciation in coal-fired derived flue gas.

#### Objective:

In order to study the effect of the additive  $\text{CaBr}_2$  content, the Ontario Hydro Method (OHM) method has been applied to analyze the mercury speciation at the entrance and export of denitration (SCR).

#### Method:

Density Functional Theory (DFT) has been used to study the adsorption of mercury halide on unburned carbon surface.

#### Result:

The results show that along with the increasing amount of additive  $\text{CaBr}_2$ , there is an increasing trend of the ratio of  $\text{Hg}^{2+}$  in flue gas.

#### Conclusion:

$\text{CaBr}_2$  addition contributes to oxidize  $\text{Hg}^0$  to  $\text{Hg}^{2+}$  and increase the mercury concentration through SCR. DFT results indicate that the adsorption of  $\text{HgBr}$  and  $\text{HgBr}_2$  on unburned carbon surface is chemisorption, and Br-C bond is stronger than Hg-C bond, both these bonds are covalent interaction.

**Keywords:** Additive  $\text{CaBr}_2$ , Mercury speciation, Flue gas, DFT, AIM, Ontario Hydro Method (OHM).

## 1. INTRODUCTION

The poisonous and heavy metal of mercury is a global pollutant, which endangers ecological environment and the health of human [1]. Coal combustion is the major anthropogenic source of the mercury emission, and the estimated 3400 tons of mercury emitted from coal-fired power plants in 2010 year [2 - 4]. The deep research of reaction and migration mechanisms of mercury in coal-fired power plants flue gas and fly ash is of great significance to effectively control mercury emission.

There is a certain amount of mercury in coal, which emissions into flue gas in burning. Along with the combustion of coal, almost mercury emitted in the form of gaseous elemental ( $\text{Hg}$ ). In the furnace flue tail, the elemental mercury ( $\text{Hg}^0$ ) is oxidized to divalent mercury ( $\text{Hg}^{+2}$ ) with the decreasing of flue gas temperature. Elemental and divalent mercury may adsorb on unburned carbon and then convert into particulate mercury ( $\text{Hg}_p$ ) [5 - 8]. In the progress of coal

\* Address correspondence to this author at the School of Energy and Power Engineering, North China Electric Power University, Baoding, China, Tel: 18331121421; Emails: 394890445@qq.com; 18331121421@163.com

combustion, the enrichment and distribution form of mercury species were affected by many factors, such as types and composition of coal, characteristics of fly ash, composition of flue gas, operation conditions of boiler and burning temperature. In detail, the content of gas  $\text{Hg}^{2+}$  is higher than  $\text{Hg}_p$  in bituminous coal flue gas, but in sub-bituminous coal flue gas, the content of gas  $\text{Hg}^0$  and  $\text{Hg}_p$  are both high, which the reasons may be the component of flue gas and fly ash in the bituminous coal has strong oxidation to  $\text{Hg}^0$ , and the constituents of flue gas and fly ash in sub-bituminous coal has strong adsorption to  $\text{Hg}^0$ . Mercury species present enrichment state on the fly ash surface, the smaller particle size of fly ash, the larger specific surface area of ash particle, and the more mercury adsorbed on ash particle. In addition, the pore structure of ash particle affects the adsorption capacity of mercury, in which the large porosity is advantageous to mercury adsorption. Active inorganic chemical component in fly ash plays an important facilitating role in mercury oxidation and capture. Ghorishi [9] revealed that the  $\text{Fe}_2\text{O}_3$  has strong oxidation to  $\text{Hg}^0$ , but the  $\text{Al}_2\text{O}_3$ ,  $\text{SiO}_2$  and  $\text{CaO}$  have relatively few oxidation to  $\text{Hg}^0$ . Moreover, transition metal oxides of  $\text{CuO}$  and  $\text{MnO}_2$  also have promoting effect on mercury oxidation [10, 11]. Gaseous  $\text{SO}_x$  as a major component of flue gas, it also affects mercury oxidation. Preso [12] proposed that  $\text{SO}_3$  has strong inhibitory effect on mercury capture in the condition of low concentration of  $\text{SO}_3$ , which the reason is the competitive adsorption between  $\text{SO}_3$  and  $\text{Hg}^0$  on active sites. Diamantopoulou [13] considered that  $\text{SO}_2$  can promote the mercury capture by fly ash due to the  $\text{SO}_2$  which increases sulfur contained active sites on active carbon. Many studies have been conducted on the effect of halogen promoting mercury oxidation, confirming that chlorine, presented as  $\text{HCl}$ ,  $\text{Cl}_2$  or  $\text{Cl}$  radicals in the flue gas, contributes to  $\text{Hg}^0$  oxidation [14]. Agarwal [15] investigated the influence of  $\text{H}_2\text{O}$ ,  $\text{SO}_2$  and  $\text{NO}$  on  $\text{Hg}^0$  oxidation when the  $\text{Cl}_2$  as oxidant, the results showed that the  $\text{H}_2\text{O}$ ,  $\text{SO}_2$  and  $\text{NO}$  make inhibition effect on  $\text{Hg}^0$  oxidation. The  $\text{HCl}$  content is considered a vital factor that affects the mercury oxidation. Ochiai [16] studied the influence of  $\text{HCl}$  on mercury adsorption on active carbon surface based temperature programmed desorption experiment, the experimental results indicated that  $\text{HCl}$  presents promoting effect on mercury adsorption, and  $\text{HCl}$  concentration plays an important role in mercury species distribution, which may be the reasons for the formation of  $\text{HgCl}_2$  by direct reaction between  $\text{HCl}$  and  $\text{Hg}^0$  or indirect reaction between  $\text{HCl}$  and  $\text{HgO}$ . Moreover, Galbreath [5] investigated the influence of  $\text{HCl}$  on mercury species transformation by injecting  $\text{HCl}$  into various flue gas which produced by burning bituminous coal, sub-bituminous coal and lignite, the experimental results showed that the injected  $\text{HCl}$  prominently promotes oxidation of  $\text{Hg}^0$  to  $\text{Hg}^{2+}$  in sub-bituminous coal flue gas, but the injected  $\text{HCl}$  promotes oxidation of  $\text{Hg}^0$  and  $\text{Hg}^{2+}$  to  $\text{Hg}_p$  in lignite flue gas. The same effect is also detected with bromine since  $\text{Cl}$  and  $\text{Br}$  are congeners sharing similar properties [17].  $\text{Br}$  can promote mercury oxidation and have the highest oxidation capability than  $\text{Cl}$  and other halogen [18 - 19]. In detail, Cao [18] researched the oxidation ability of  $\text{HF}$ ,  $\text{HCl}$ ,  $\text{HBr}$  and  $\text{HI}$  to  $\text{Hg}$  based the sub-bituminous coal flue gas, the results showed that oxidation ability are  $\text{HBr} > \text{HI} \gg \text{HCl} \sim \text{HF}$ , a little added  $\text{HBr}$  in flue gas can make a contribution to 90% mercury oxidation rate. Liu [19] studied the synergism effect of  $\text{Br}_2$  and fly ash on mercury oxidation, the results showed that  $\text{Br}_2$  can facilitate the mercury oxidation, but  $\text{Br}_2$  mixed with fly ash especially for unburned carbon that can remarkably promote the mercury oxidation. The added bromine promotes mercury adsorption on fly ash and unburned carbon particle, and then facilitates heterogeneous oxidation reaction. In addition, the bromine salt is easier to decompose for participation in mercury oxidation. Comparing with the study of the effect of chlorine, there are still scarce conducted on  $\text{Br}$ , especially in field experiments. Also, SCR catalyst is another important factor in this process, promoting mercury oxidation as well as providing adsorption sites. Unburned carbon can provide active sites for the adsorption of bromine and mercury [20, 21], which promotes the oxidation of elemental mercury.

In the flue gas, mercury presents three forms which are element mercury, divalent mercury and particulate mercury. Particulate mercury ( $\text{Hg}_p$ ) does not have water-solubility and it can be removed by dust control equipment. Divalent mercury ( $\text{Hg}^{2+}$ ) is soluble in water and it can be removed by wet flue gas desulfurization devices. Elemental mercury

Hg<sup>0</sup> is not soluble in water and difficult to be removed [8, 22, 23]. Therefore, promoting the Hg<sup>0</sup> convert into Hg<sup>2+</sup> and Hg<sub>p</sub> is beneficial ecologically and has been the research focus of domestic and abroad scholars.

To sum up, the previous studies mostly focused on the effect of HCl or HBr on mercury oxidation and were carried out in simulated flue gas, there have been not enough researches on the contribution of CaBr<sub>2</sub>, as well as the oxidizing action on mercury of additives with different concentrations. Stated thus, in order to study the influence of additive CaBr<sub>2</sub> on mercury speciation in flue gas, the additives experiment was carried out based on one 300 MW coal-fired boiler, the Ontario Hydro Method (OHM) was utilized to sample mercury at the denitration entrance and export., and the variation of mercury before and during adding the additives was captured and the effect of the additives was analyzed. In addition, Density Functional Theory (DFT) computational study was used to theoretically analysis mercury oxidized by bromine on unburned carbon surface.

## 2. EXPERIMENTAL AND COMPUTATIONAL DETAILS

### 2.1. Experimental Condition

The CaBr<sub>2</sub> addition experiments were conducted in one 300MW boiler of #1 unit in the power plant, whose annual power generation is 6~8 billion kW·h. This 4×300MW unit plant adopts first medium reheating natural circulation drum boiler under subcritical pressure, equipped with the pollution control facilities and installations, such as the electrostatic precipitator, SCR denitrification and desulfurization devices, etc.

Sampling points were set at SCR entrance and export as shown in Fig. (1). CaBr<sub>2</sub> was fed with a screw feeder to vibration coal feeder. The flue gas was extracted from sampling points for thirty minutes for mercury collecting. At SCR entrance and export sampling points, the Ontario Hydro Method (OHM) [24] was applied. The ash particles were permeated *via* a heated quartz filter membrane, and then passed through three adsorbing bottles in turn, which one is 1 mol/L KCl solution, one with 10% H<sub>2</sub>O<sub>2</sub>-5% HNO<sub>3</sub> solution and another one is 4% KMnO<sub>4</sub>-10% H<sub>2</sub>SO<sub>4</sub> solution. These solutions were used to adsorption for Hg<sup>2+</sup> and Hg<sup>0</sup>. And the absorption liquid was taken back to the laboratory immediately for digestion and finally was collected in Teflon bottles. The RA-915 type mercury analyzer of LUMEX company was used for measuring mercury content in all the samples.

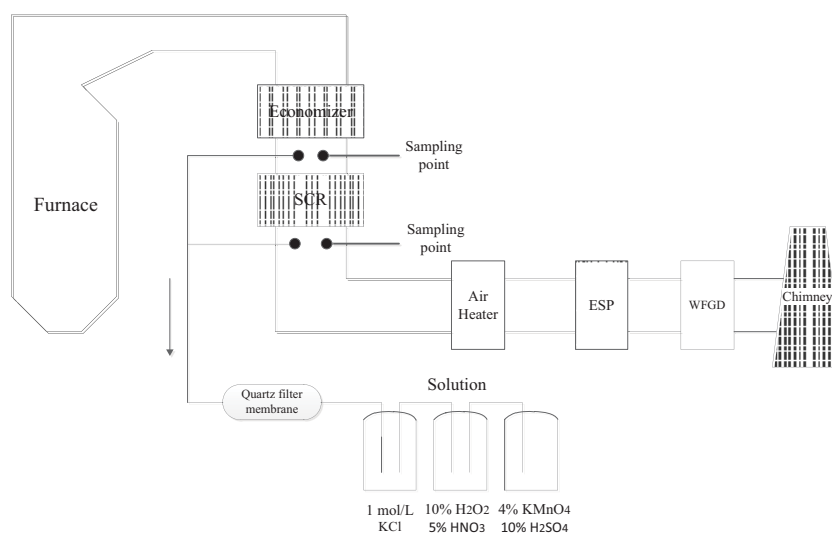


Fig. (1). CaBr<sub>2</sub> addition experiments schematic.

Serial numbers C1 to C6 represent condition one to condition six, respectively. In detail, there is no CaBr<sub>2</sub> addition in C1. From C2 to C6, the amount of CaBr<sub>2</sub> increases gradually and the specific dosage is shown in Table 1. Proximate analysis and mercury content of coal sample are shown in Table 2.

**Table 1.** CaBr<sub>2</sub> addition amount.

Conditions	C1	C2	C3	C4	C5	C6
CaBr <sub>2</sub> addition amount(kg/h)	0	0.5	1.5	5	15	50

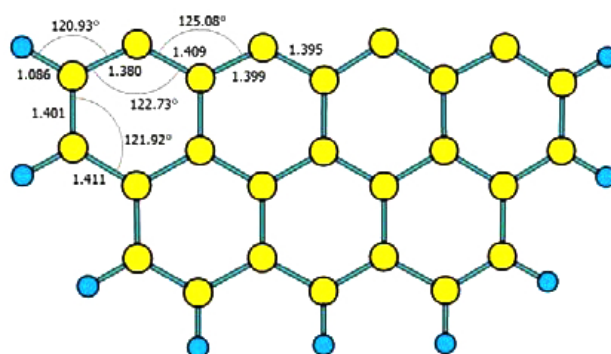
**Table 2.** Proximate analysis and mercury content of coal.

Moisture	Ash(A <sub>ar</sub> )	Volatility(V <sub>ar</sub> )	Fixed carbon(FC <sub>ar</sub> )	Mercury(ng/g)
15.56	10.52	28.92	41.16	46.8

## 2.2. Computational Details

Single layer graphene model was used to simulate unburned carbon surface, which has been proven that it provides satisfactory results for relevant reaction mechanisms of carbon based surface [25, 26]. As shown in Fig. (2), seven-ring benzene cluster model of Zigzag was applied to simulate unburned carbon in flue gas in this paper, and the active sites of this model were not saturated by hydrogen. Density functional theory B3LYP method [27] was used to the optimization of configuration and calculation of energy. In detail, pseudopotential basis set SDD was used to mercury atom, and the Pople 6-31G(d) basis set was applied for non-metal elements (C, H and Br) [25]. In this paper, all of the calculation was carried out by Gaussian 09 program [28]. The adsorption energy was calculated by equation (1):

$$E_{ads} = E_{model+adsorbate} - E_{model} - E_{adsorbate} \quad (1)$$

**Fig. (2).** Seven-ring benzene cluster model.

Yellow and blue ball represent carbon and hydrogen atom, respectively.

Where  $E_{model+adsorbate}$  is the total energy of adsorption complex of benzene cluster model and adsorbate,  $E_{model}$  and  $E_{adsorbate}$  are the energy of benzene cluster model and adsorbate, respectively. Negative value of  $E_{ads}$  represents the adsorption progress is exothermic, and higher negative values of  $E_{ads}$  reflects the stronger adsorption capacity of benzene cluster model onto adsorbate [29, 30].

In addition, Atoms in Molecules (AIM) method [31, 32] was used to analyze the type and strength of bond between unburned carbon model and adsorbates. AIM was evaluated by wave function analysis program of Multiwfn 3.2.1 [33], and isosurface maps of adsorption complexes were plotted by VMD program in this paper [34].

## 3. RESULTS AND DISCUSSION

### 3.1. Effect of CaBr<sub>2</sub> Addition on Mercury Speciation at SCR

The concentrations of gaseous mercury at the SCR entrance and export in different experimental conditions are shown in Table 3. It is clearly observed that before entering SCR, mercury is mainly presented as Hg<sup>0</sup> in the flue gas, which has been confirmed by S. Niksa [35].

Table 3. Gaseous mercury concentration at SCR in different conditions.

Condition	Addition Amount (kg/h)	Measuring Position	Hg (g) Concentration (ug/m <sup>3</sup> )	Hg <sup>2+</sup> (g) Concentration (ug/m <sup>3</sup> )
C1	0	Entrance	8.26	0.83
		Export	1.38	3.21
C2	0.5	Entrance	2.42	0.32
		Export	2.71	1.69
C3	1.5	Entrance	1.22	0.34
		Export	2.04	2.64
C4	5	Entrance	0.91	0.43
		Export	0.95	4.54
C5	15	Entrance	0.83	0.46
		Export	0.38	5.24
C6	50	Entrance	1.04	0.44
		Export	0.59	2.59

In Table 2 it can be found that the mercury mass fraction is 46.8 ng/g, and mercury exists in three forms: elemental mercury, divalent mercury and particle mercury. During the combustion of coal, variant mercury species decompose and release gaseous mercury into flue gas. Lopez-Anton [36, 37] demonstrated that HgCl<sub>2</sub>, HgS, HgO and HgSO<sub>4</sub> are the main mercury species in coal-fired ash and gas. In detail, the thermal decomposition temperature of HgCl<sub>2</sub> is 70°C. There are two different forms of crystal structure, black cube HgS and red six party HgS, which decompose at the temperature of 170°C and 240°C, respectively, the component HgO and HgSO<sub>4</sub> decompose at the temperature of 200°C and 500°C. In addition, mercury species of Hg<sub>2</sub>SO<sub>4</sub> and Hg<sub>2</sub>Cl<sub>2</sub> also exist in ash and flue gas, but Hg<sub>2</sub>SO<sub>4</sub> and Hg<sub>2</sub>Cl<sub>2</sub> are unstable.

In condition one in Table 3, in which the gaseous Hg<sup>0</sup> and Hg<sup>2+</sup> concentrations are 8.26 μg/m<sup>3</sup> and 0.83 μg/m<sup>3</sup>, respectively, it means mercury mainly exists in Hg<sup>0</sup> form. In detail, the mercury component Hg<sub>2</sub>SO<sub>4</sub> easily decomposes to Hg and HgSO<sub>4</sub>, Hg<sub>2</sub>Cl<sub>2</sub> easily decomposes to Hg and HgCl<sub>2</sub>, as shown in equations (2) and (3):



Similarly, the HgCl<sub>2</sub>, HgS, HgO and HgSO<sub>4</sub> in fly ash and flue gas decompose into element mercury and other substance at high temperature. Along with the temperature of flue gas decreases, the decomposition of almost mercury species is halted, and mercury oxidation dominates gradually. Due to the halogen and sulfur consist in flue gas, the homogeneous oxidation reaction of element mercury to oxidized mercury are occurred, such as shown in equations (4) to (7) [38].



Where the (g) represents gaseous phase. Hg<sup>0</sup> can be oxidized to HgCl by gaseous HCl and Cl<sub>2</sub>, and then some HgCl be oxidized completely to HgCl<sub>2</sub>. In addition, heterogeneous oxidation reactions between chlorine and element mercury on ash particle are shown in equations (8) to (11) [39].





Where the (ad) represents substance adsorbed on ash or unburned carbon particle.

In addition,  $\text{Hg}^0$  also can be oxidized by sulfur. Rubel demonstrated that a good correlation exists between sulfur and mercury capture. He proposed that the unburned carbon released from high sulfur coals have shown to have higher mercury adsorption capacity than that from low sulfur coals.  $\text{H}_2\text{S}$  and  $\text{SO}_2$  play an important role in oxidizing mercury in flue gas, the detailed oxidation reaction as shown in equations (12) to (14) [40].



$\text{H}_2\text{S}$  can be oxidized to  $\text{S}^0$  by oxygen or  $\text{SO}_2$  on ash or unburned carbon surface, and then adsorbed sulfur can capture  $\text{Hg}^0$ , and finally,  $\text{HgS}$  may adsorb on ash surface to form particle mercury or releases into flue gas to form gaseous oxidized mercury. To sum up, the massive element mercury and a little oxidized mercury released during the coal combustion, so the  $\text{Hg}^0$  concentration is larger than  $\text{Hg}^{2+}$  concentration at the SCR entrance. Along with the temperature of flue gas decreased, the oxidation of mercury is dominant than decomposition, so the  $\text{Hg}^{2+}$  concentration is larger than  $\text{Hg}^0$  concentration at the SCR export.

In each condition, there is an increase of  $\text{Hg}^{2+}$  and conversely, a decrease of  $\text{Hg}^0$  in flue gas at SCR export compared with entrance, which means the oxidation of  $\text{Hg}^0$  to  $\text{Hg}^{2+}$  taken place in the SCR. Almost all of the mercury leaving furnace is presented in element form in flue gas with high temperature, whose oxidation from the elemental form to divalent form takes place as the temperature decreases and gets promoted under the effect of halogen in the coal and SCR catalyst. Divalent mercury is more strongly adsorbed on the surface of both ash particles and SCR catalyst than element mercury [41]. As clearly shown in C1 in Table (3), the increase of gaseous divalent mercury amount in the flue gas is less than that of decrease of gaseous element mercury and the total gaseous mercury concentration through SCR, which the reasons may be that the gaseous  $\text{Hg}^{2+}$  adsorbed on unburned carbon and SCR catalyst surface. With the additive  $\text{CaBr}_2$  has been added in C2, the  $\text{Hg}^0$  and  $\text{Hg}^{2+}$  concentration decreased in SCR entrance which compared with C1. The  $\text{Hg}^0$  concentration decreased which dues to the oxidation of  $\text{Hg}^0$  to  $\text{Hg}^{2+}$  by  $\text{CaBr}_2$ , but the  $\text{Hg}^{2+}$  concentration did not increase but decrease, which the reasons may be that the  $\text{CaBr}_2$  promotes the adsorption of  $\text{Hg}^{2+}$  on unburned carbon surface. In addition, the  $\text{Hg}^{2+}$  concentration in SCR export is higher than that in SCR entrance in C2, which means that the SCR catalyst can promote the oxidation of  $\text{Hg}^0$  to  $\text{Hg}^{2+}$ . From C2 to C5, as  $\text{CaBr}_2$  addition amount increases, the proportion of  $\text{Hg}^{2+}$  increases as well both at SCR entrance and export, at the same time, the  $\text{Hg}^0$  proportion decreases at SCR entrance, experimental results indicate that  $\text{CaBr}_2$  can facilitate the oxidation of  $\text{Hg}^0$  to  $\text{Hg}^{2+}$  in general. Especially, C5 reached the extreme point among these conditions and although more  $\text{CaBr}_2$  was added in C6, the proportion of  $\text{Hg}^{2+}$  in C5 is larger than that of C6 both at SCR entrance and export, the reason of which is mainly that the  $\text{CaBr}_2$  addition amount has reached a saturation value beyond and thus the oxidation is no longer enhanced [4, 42].

Fig. (3) shows the variation of  $\text{Hg}$  and  $\text{Hg}^{2+}$  concentration decrease rate at SCR entrance alone with the increase of  $\text{CaBr}_2$  addition amount. As shown in Fig. (3), with the additive  $\text{CaBr}_2$  has been added, the gaseous  $\text{Hg}$  concentration decreased. In C2,  $\text{CaBr}_2$  with addition level of 0.5 kg/h was added in flue gas, the reduction rate of gaseous  $\text{Hg}^0$  concentration at SCR entrance is 70.7% comparing with that of C1. Similarly, the reduction rates of gaseous  $\text{Hg}^0$  of C3, C4, C5 and C6 are 85.2%, 89.0%, 90.6% and 87.0%, respectively. Analyzing these reduction rates of different conditions, it can be found that the gaseous mercury concentration decrease rapidly along with the increase of  $\text{CaBr}_2$  addition level in general, which indicates that additive  $\text{CaBr}_2$  can oxidize  $\text{Hg}^0$  to  $\text{Hg}^{2+}$ , these findings agree with previous studies [43, 44]. Interestingly, along with the increase of  $\text{CaBr}_2$  addition amount, the gaseous  $\text{Hg}^{2+}$  concentration is not increase but decrease at the SCR entrance, the reasons may be that the additive  $\text{CaBr}_2$  contributes to more fly ash in flue gas, and more oxidized  $\text{Hg}^{2+}$  adsorb on ash particles, which makes the decrease of  $\text{Hg}^{2+}$  concentration at SCR entrance.

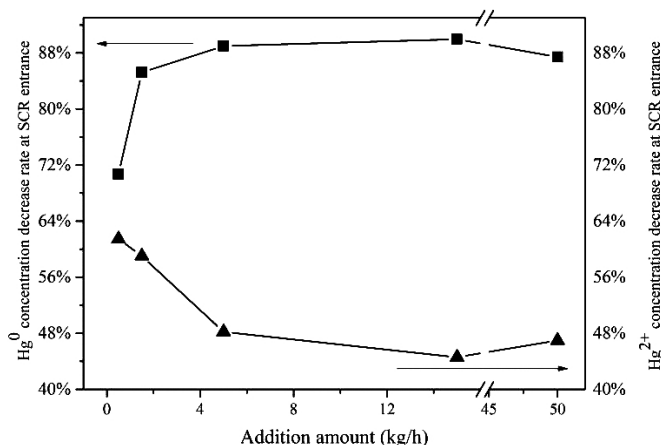


Fig. (3). Variation of Hg<sup>0</sup> and Hg<sup>2+</sup> concentration decrease rate at SCR entrance versus CaBr<sub>2</sub> addition amount.

Fig. (4) shows the variation of Hg<sup>2+</sup> concentration increase rate at SCR export along with the increase of CaBr<sub>2</sub> addition amount. As shown in Fig. (4), whether or not to add additive CaBr<sub>2</sub>, the gaseous Hg<sup>2+</sup> concentration all increased. In C1 which there is no CaBr<sub>2</sub> addition, the increase ratio of Hg<sup>2+</sup> concentration between SCR export and entrance has reached to 74%, probably because that in C1, with quite little halogen in coal and the subsequent in flue gas, almost all the mercury oxidation is conducted in SCR while halogen contributes to mercury oxidation. Along with the increase of CaBr<sub>2</sub> addition amount, the increase rate of Hg<sup>2+</sup> concentration also increases, and in C5 which the CaBr<sub>2</sub> addition amount is 15 kg/h, the increase rate reaches the maximum value, which indicates that the oxidation reaction is saturated. In C6, with the CaBr<sub>2</sub> addition amount continues to increase to 50 kg/h, the Hg<sup>2+</sup> concentration increase rate has decreased to 82.4%.

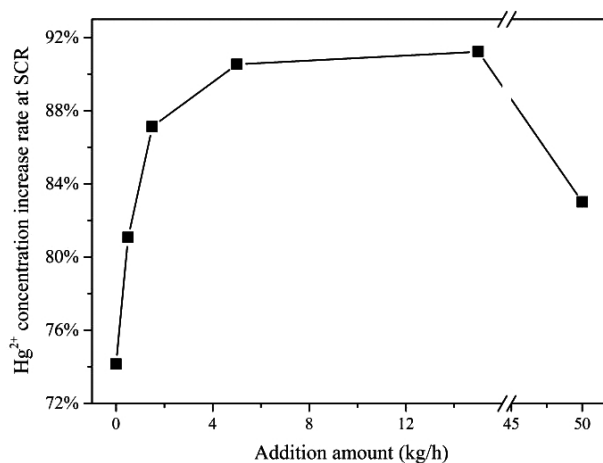


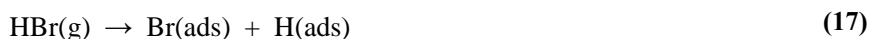
Fig. (4). Variation of Hg<sup>2+</sup> concentration increase rate at SCR versus CaBr<sub>2</sub> addition amount.

The subsequent products such as CaO and Ca(OH)<sub>2</sub> may be produced because of CaBr<sub>2</sub> addition as shown in equation (15) to (16), and these subsequent products are effective of Hg<sup>2+</sup> adsorbents. Flue gas leaving the furnace with high temperature, bromine is presented mainly as HBr [41], and as the gas temperature decreases, Br atoms are in a concentration [4] and in the subsequent cooling process Br<sub>2</sub> is formed. Therefore in the flue gas leaving the furnace before entering SCR, HBr is the most speciation of bromine. In addition, the HBr released from the reaction of CaBr<sub>2</sub> and H<sub>2</sub>O, the reaction as shown in equations (15) and (16).



Both homogeneous and heterogeneous chemistry exist in Hg<sup>0</sup>(g) oxidation. In the flue gas, according to what

Stephen [4] has found,  $\text{Hg}^0$  is first partially oxidized by Br atom into HgBr and then oxidized into  $\text{HgBr}_2$  by  $\text{Br}_2$ . Since the concentration of  $\text{Br}_2$  is smaller than that of Br atoms in high temperature flue gas, homogeneous oxidation results in most mercury being presented as HgBr(g) with a small amount of  $\text{HgBr}_2$ . Gao [23] proposed that in the flue gas leaving the furnace before entering SCR, most bromine is presented in HBr and a small part in Br atoms with tiny amount of  $\text{Br}_2$ . Stephen [4] presented that Hg homogeneous chemistry with Br species is much faster than with Cl species because the Br atom concentrations at the furnace exit are three to four orders of magnitude greater, the dominant channels with Br are analogous to those for Cl, whereby a Br atom partially oxidizes  $\text{Hg}^0$  into HgBr. In addition, mercury also oxidizes heterogeneously on unburned carbon with Br species. Raik [41] suggested that in the subsequent cooling process, the fuel bromine or added bromine is eventually transformed into HBr. Based on the DFT calculation, Padak's [47] results for Hg adsorption in the presence of chlorine, it was found that HgBr species are more stable on the unburned carbon surface than  $\text{HgBr}_2$  species. Fujiwara [35] proposed that heterogeneous  $\text{Hg}^0$  oxidation on unburned carbon is usually the essential inherent mechanism to oxidize  $\text{Hg}^0$  in coal-derived flue gas. Bench-scale experiments [45] and quantum chemistry theoretical studies [46] have indicated that heterogeneous mercury oxidation is at least 90% proportion of the overall oxidation in coal-fired flue gas. Heterogeneous reaction is mainly determined by adsorption on Unburned Carbon (UBC) surfaces, and the oxidation mechanism is as follows:



Where (g) and (ads) represents gaseous and adsorption state, respectively [4].

Since most bromine is in HBr form in the high temperature gas, which is easily adsorbed on unburned carbon surface *via* equation (17). And then, gaseous element mercury is adsorbed on carbon surface through the interaction with Br(ads). In addition, HgBr(ads) may be oxidized further into  $\text{HgBr}_2(\text{ads})$  by gaseous HBr. Padak [47] confirmed that HgBr is more strongly and stably adsorbed on the unburned carbon surface than  $\text{HgBr}_2$  by quantum chemistry calculation. Gale *et al.* [48] found that the Ca enhances mercury capture by preventing  $\text{Hg}^{2+}$  desorption from carbon surface. Therefore, due to homogeneous and heterogeneous chemistry, in the high temperature gas before entering SCR, mercury presented mainly in HgBr form, most of which is adsorbed on UBC surface.

According to the Deacon reaction:  $4\text{HCl} + \text{O}_2 \rightarrow 2\text{H}_2\text{O} + 2\text{Cl}_2$ , when the flue gas enters SCR,  $\text{Cl}_2$  is produced under the effect of the vanadium-based catalyst. There has been no specified reaction in bromine situation and it is predicted here that the concentration of  $\text{Br}_2$  begins to increase in SCR as flue gas temperature decreases [4]. Both the homogeneous and heterogeneous mercury oxidations exist in SCR. According to Hein [41], homogeneous mercury oxidation in SCR involves  $\text{Hg}^0(\text{g})$  reacting with HBr to produce  $\text{HgBr}_2(\text{g})$ . Since mercury in the flue gas entering SCR is mainly in HgBr(ads) form, no big  $\text{Hg}^0(\text{g})$  concentration variation is supposed to be detected. Mercury oxidation in SCR is mainly in heterogeneous chemistry [39].

The produced  $\text{Br}_2$  in SCR is a strong oxidant and can easily oxidize adsorbed HgBr into  $\text{HgBr}_2$  which then gets desorbed. Also the remained HBr may react with HgBr(ads) to form  $\text{HgBr}_2(\text{g})$  *via* equation (20) [4] and therefore  $\text{Hg}^{2+}(\text{g})$  concentration in SCR increases.



On the other hand, two reaction mechanisms have been previously proposed for mercury heterogeneous oxidation on vanadium-based SCR catalyst surface. Senior [49] applied Eley-Rideal mechanism which indicates that adsorbed mercury on catalyst surface reacts with hydrogen halide in the flue gas, while Hein *et al.* [41] have mentioned Langmuir-Hinshelwood mechanism that  $\text{Hg}^0$  and hydrogen halide both are adsorbed on catalyst surface firstly, and then start to react. When hydrogen halide concentration is much larger than element mercury, mercury oxidation on the SCR catalyst surface is mainly dominated by Langmuir-Hinshelwood mechanism because of the higher affinity of hydrogen halide with the active sites in SCR catalyst than mercury [50]. Therefore compared to HBr in the flue gas, there are not much  $\text{Hg}^0$  and  $\text{Hg}^{2+}$  adsorbed on SCR catalyst surface. Abad-Valle *et al.* [51] found that hydrogen halide binds itself to carbon particle surface prior to Hg, indicating that not much  $\text{Hg}^{2+}(\text{g})$  is adsorbed on unburned carbon surface. Through analyzing heterogeneous and homogeneous mercury oxidation and adsorption on the unburned carbon and SCR catalyst

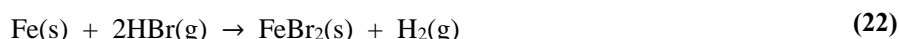
surface, it is shown that CaBr<sub>2</sub> addition contributes to an increase of element mercury transform into divalent mercury.

The dominant forms of Hg in coal-fired flue gas are Hg<sup>0</sup> and Hg<sup>2+</sup> [52], and the fraction of Hg<sup>2+</sup> in flue gas depends on the coal quality, boiler loads and so on. Hg<sup>0</sup> can be oxidized to HgCl and HgCl<sub>2</sub> by Cl<sub>2</sub> and HCl, respectively. HCl is the major Cl species under the condition of SCR operation [4]. HCl is more stably adsorbed on SCR catalyst surface than Hg, which means that the HCl inhibits the mercury adsorption on catalyst surface [53]. Generally, element mercury on SCR catalyst oxidizes faster than that on unburned carbon under the condition of chlorine level is moderate or higher.

Since the unburned carbon can enhance mercury capture, different coal ranks with dissimilar unburned carbon content in flue gas have different results in mercury capture. The combustion results of anthracites coal and bituminous coal show that the unburned carbon in fly ash is anisotropic, unresolved and dense. On the contrary, the structure of unburned carbon in fly ash is isotropic and porous, which formed from subbituminous or lignite. The different characteristics of unburned carbon greatly affect the mercury capture, the UBC with anisotropic fused structure is more favorable for adsorbing mercury. Gale [48] found that much more mercury oxidation can be realized by blending coal, even though there was less chlorine. The reasons may be that the added bituminous coal yields more unburned carbon in the ash, which enhances mercury oxidation. In addition, low-rank coal with high concentration of calcium can promote mercury oxidation. Gale [48] proposed that calcium can enhance the HgCl adsorption on the unburned carbon surface and element mercury adsorption onto chlorinated-carbon sites.

Temperature affects mercury capture *via* the unburned carbon formation in the boiler with high temperature to the quenching environment of flue gas. In addition, homogeneous Hg oxidation by Br begins as the flue gas cools below 600°C [4]. Subtle changes in boiler operation condition can potentially results in significant changes for unburned carbon properties [54], and these changes may impact mercury capture in fly ash.

It is well known that chlorine can cause serious corrosion to boilers, heater exchangers and pipes surface as a result of complex chemical interactions between species like HCl, Cl<sub>2</sub>, H<sub>2</sub>O, O<sub>2</sub> and metal [55, 56]. Similar to chlorine-associated corrosion, bromine may cause corrosion depending on the flue gas conditions. Element bromine is injected *via* the addition of CaBr<sub>2</sub>, and HBr is the primary Br species in the gas phase and little Br<sub>2</sub> may be present at higher temperature. Both the HBr and Br<sub>2</sub> can react with metal to form metal bromides. The oxidation mechanisms can be revealed *via* the equation (21) to (26) [57].



Stated thus, the CaBr<sub>2</sub> addition has caused corrosion to the metal of boiler, which makes the negative effect on the stable operation of heat exchange pipes. The present of HBr and Br<sub>2</sub> can thin the pipe walls and reduce the structural strength of metal pipes. Although the additive CaBr<sub>2</sub> can promote the mercury oxidation, the corrosion characteristic of HBr which formed from CaBr<sub>2</sub> also should be considered.

### 3.2. DFT Calculations

In order to gain further insight into the adsorption mechanisms of mercury and halogen on the unburned carbon surface, the reaction path of Hg on Zigzag carbon model which adsorbed single bromine atom has been studied, in addition, the adsorption complex of Zigzag···HgBr<sub>2</sub> has been optimized.

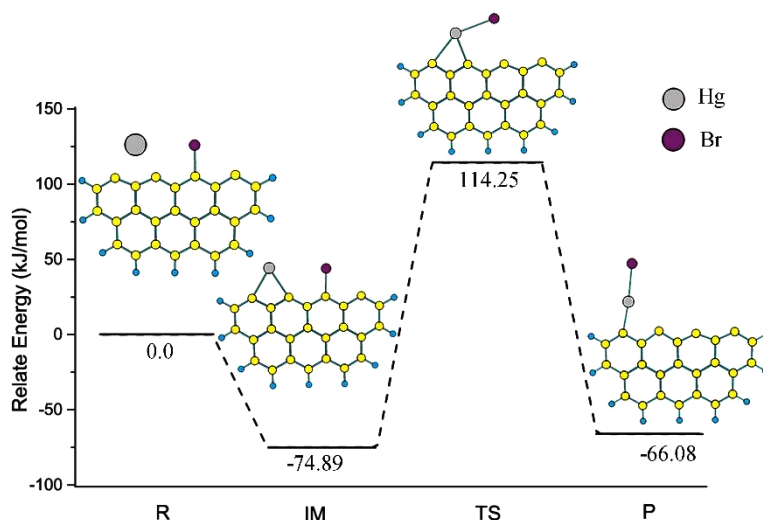


**Fig. (5).** The reaction path of Hg and C<sub>25</sub>H<sub>9</sub>-Br model.

R, IM, TS and P represents reaction, intermediate, transition state and product.

According to the Equation (18), the generation path of adsorbed HgBr *via* gas Hg and Zigzag-Br model has been shown in Fig. (5). Gas element mercury chemically adsorbed on active sites which on the side of Br atom, and corresponding adsorption energy is 74.89 kJ/mol. In transition state structure of TS, the bond between active site and Br atom broken, and the Br atom closed to the adsorbed Hg atom. The structure of TS is not stable and corresponding energy is higher 114.25 kJ/mol than that of reactants. TS quickly converts into final product along with the Br atom far away from active sites. The total energy of final product is lower 66.08 kJ/mol than that of the reactants. The theoretic DFT results have verified the validity of Equation (18) and indicated that the adsorption of gas Hg<sup>0</sup> on carbon model which adsorbed Br is chemisorption.

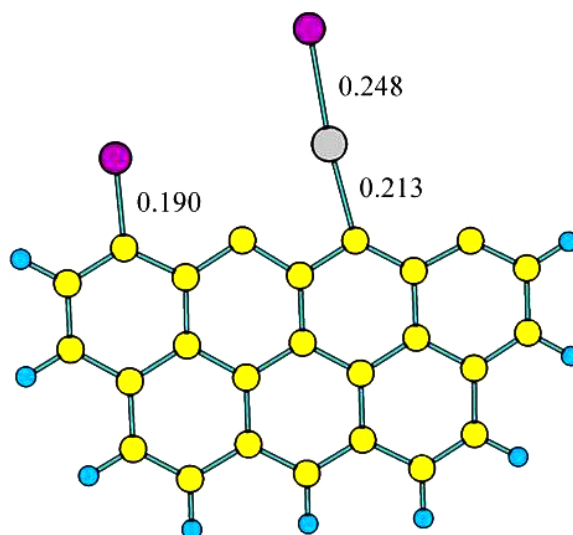


**Fig. (6).** The adsorption configuration of HgBr<sub>2</sub> on C<sub>25</sub>H<sub>9</sub> model.

The optimization complex of HgBr<sub>2</sub> adsorbed on Zigzag carbon model surface is shown in Fig. (6). One of the Hg-Br bond broken, Br atom and Hg atom adsorbed on active sites, respectively. The adsorption energy of HgBr<sub>2</sub> on Zigzag carbon model surface is 325.46 kJ/mol, indicates that the adsorption is chemisorption. As shown in Fig. (4), the bond length of Br-C and Hg-C is 0.190 nm and 0.213 nm, respectively, the bond strength of Br-C may stronger than that of Hg-C. This adsorption configuration may be formed *via* the oxidation reaction of Br atom and Zigzag -HgBr complex.

Atoms in Molecules (AIM) theory has been successfully and widely used to study the properties of shared-shell (covalent) and closed-shell bonding [58, 59]. This theory depicts that the Hessian matrix of the charge density can be well applied to evaluate characterize of a bond. The bond critical point (BCP) is the laplacian of the charge density  $\nabla^2\rho(r)$ , which is the sum of three eigenvalues of Hessian matrix. According to the criteria proposed by Carroll and Bader [60, 61] based on charge density topology, there are some regulations can be used to analysis the bond characterize. First, the presence of BCP between two atoms indicates that the existence of bond path between these two atoms. Second, the value of charge density at BCP is positively correlated with the binding energy for hydrogen bond and covalent bond. Third, the positive and negative values of laplacian of the charge density at the BCP are indicative of closed-shell and covalent interaction, respectively. In addition, Cremer suggested that potential energy density  $V(r)$ , Lagranian kinetic energy  $G(r)$  and total energy density  $H(r)$  ( $H = V + G$ ) can be used to distinguish the covalent and closed-shell interaction. In detail,  $|V(r)| > G(r)$  and  $H(r) < 0$  is indicative of covalent interaction, conversely,  $|V(r)| < G(r)$  and  $H(r) > 0$  is indicative of closed-shell bonding.

The BCPs between  $\text{HgBr}$  and carbon model have been shown in Fig. (7a), which indicates that the bond paths existed between these interaction atoms. The results of charge density topological analysis have been shown in Table 4. In the configuration of  $\text{HgBr}$  adsorbed on carbon model surface, the sign of  $\nabla^2\rho(r)$  at both BCPs of  $\text{Hg-C}$  bond is positive, which indicates that the bonding between  $\text{Hg}$  atom and active site is covalent interaction. In similarly, the positive sign of  $\nabla^2\rho(r)$  of  $\text{Hg-Br}$  bond in this configuration is indicative of covalent bond. According to the Cremer's criterion, the BCP of  $\text{Hg-C}$  and  $\text{Hg-Br}$  bonds with characteristic of  $|V(r)| > G(r)$  and  $H(r) < 0$  as shown in Table 4, which demonstrated that these bonding are covalent interaction. The value of charge density  $\rho$  at the BCP of  $\text{Hg-C}_2$  bond is larger than that of  $\text{Hg-Br}$  bond, demonstrating that the bonding strength of  $\text{Hg-C}$  bond is stronger than that of  $\text{Hg-Br}$  bond. The same analysis has been conducted to the configuration of  $\text{HgBr}_2$  adsorbed on carbon model as shown in Fig. (7b), it can be concluded that the bonding of  $\text{Br}$  and  $\text{C}$  atom belongs to covalent interaction, and the  $\text{Br-C}$  bond is stronger than  $\text{Hg-C}$  and  $\text{Hg-Br}$  bonds. Analyzing the values of  $G$ ,  $V$  and  $H$ , it can be also found that these bonds are covalent interaction.

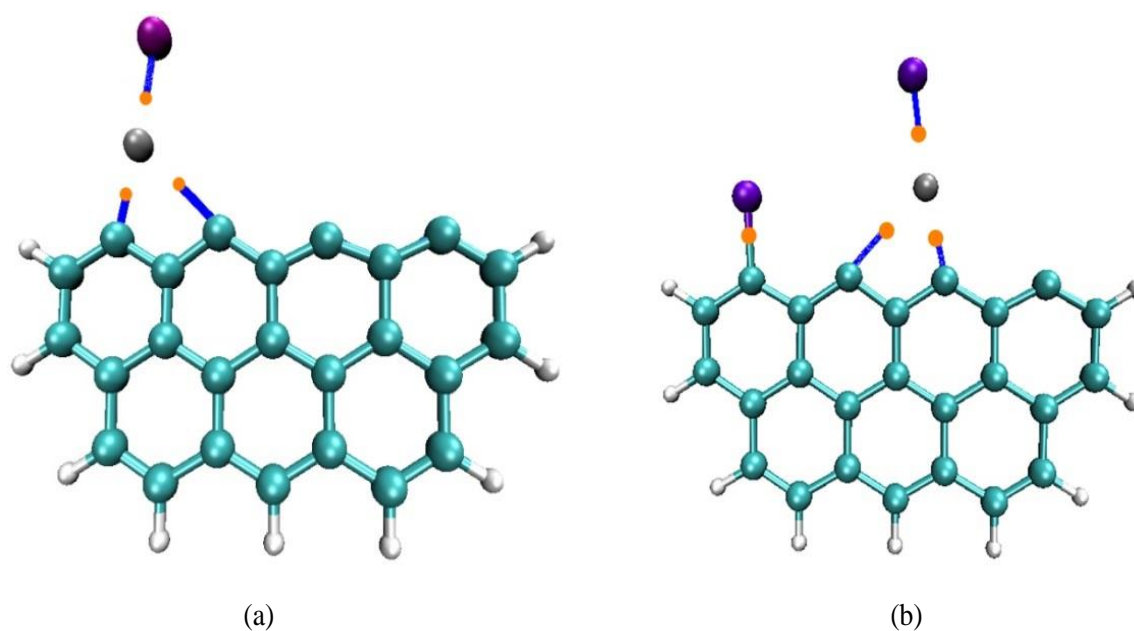


Fig. (7). Electron density topologies for (a)  $\text{HgBr-C}_{25}\text{H}_9$  complex, (b)  $\text{HgBr}_2\text{-C}_{25}\text{H}_9$  complex. Bond critical points (BCP) are shown in orange, paths are shown in blue.

Table 4. Topological parameters of the BCP of bond in adsorption configurations.

Configurations	Bond	$\rho$	$\nabla^2\rho$	G	V	H
$\text{C}_{25}\text{H}_9\text{-HgBr}$	Hg-Br	0.0811	0.1492	0.0595	-0.0818	-0.0222
	Hg-C <sub>1</sub>	0.0282	0.8266	0.0206	-0.0210	-0.0004
	Hg-C <sub>2</sub>	0.1161	0.1590	0.0862	-0.1326	-0.0464

(Table 4) contd....

Configurations	Bond	$\rho$	$\nabla^2\rho$	G	V	H
C <sub>25</sub> H <sub>9</sub> -HgBr <sub>2</sub>	Hg-Br	0.0812	0.1486	0.0595	-0.0819	-0.0224
	Hg-C <sub>1</sub>	0.1138	0.1706	0.0870	-0.1313	-0.0443
	Hg-C <sub>2</sub>	0.0311	0.0893	0.0229	-0.0235	-0.0006
	Br-C	0.1676	-0.1903	0.0578	-0.1632	-0.1054

## CONCLUSION

In one 4×300 MW coal-fired power plant, addition experiment and DFT theoretical calculation were conducted to study the effect of the CaBr<sub>2</sub> additive on mercury speciation at SCR entrance and export. Total gaseous mercury concentration through SCR increases due to the CaBr<sub>2</sub> addition, which may be the reason for HgBr oxidation and desorption under hydrogen halide condition. There is a saturation value of CaBr<sub>2</sub> addition, which makes the mercury oxidation behavior no longer enhanced. An overall effect indicates that CaBr<sub>2</sub> addition contribute to Hg<sup>2+</sup> increasing and Hg<sup>0</sup> decreasing, demonstrating the positive effect of transformation of Hg<sup>0</sup> to Hg<sup>2+</sup>. The desorption of Hg<sup>2+</sup> by HBr and Br<sub>2</sub> reacting with CaO and Ca(OH)<sub>2</sub> which is produced from CaBr<sub>2</sub> in high temperature flue gas may also be applied to explain the increase of total gaseous mercury concentration. DFT calculation results show that the bonding of HgBr and HgBr<sub>2</sub> with active sites is indicative of covalent interaction, and the Br-C bond is stronger than Hg-C bond. Both HgBr and HgBr<sub>2</sub> can stably adsorb on the unburned carbon surface.

## CONFLICT OF INTEREST

The authors declare no conflict of interest, financial or otherwise.

## ACKNOWLEDGEMENTS

This study was financially supported by the Research project of Southern Power Grid (No. K-GD2014-173).

## REFERENCE

- [1] Pacyna, E.G.; Pacyna, J.M.; Sundseth, K.; Munthe, J.; Kindbom, K.; Wilson, S.; Steenhuisen, F.; Maxson, P. Global emission of mercury to the atmosphere from anthropogenic sources in 2005 and projections to 2020. *Atmos. Environ.*, **2010**, *44*(20), 2487-2499. [http://dx.doi.org/10.1016/j.atmosenv.2009.06.009]
- [2] Pirrone, N.; Cinnirella, S.; Feng, X.; Finkelman, R.B.; Friedli, H.R.; Leaner, J.; Mason, R.; Mukherjee, A.B.; Stracher, G.B.; Streets, D.G. Global mercury emissions to the atmosphere from anthropogenic and natural sources. *Atmos. Chem. Phys.*, **2010**, *10*(13), 5951-5964. [http://dx.doi.org/10.5194/acp-10-5951-2010]
- [3] Seigneur, C.; Vijayaraghavan, K.; Lohman, K.; Karamchandani, P.; Scott, C. Global source attribution for mercury deposition in the United States. *Environ. Sci. Technol.*, **2004**, *38*(2), 555-569. [http://dx.doi.org/10.1021/es034109t] [PMID: 14750733]
- [4] Niksa, S.; Naik, C.V.; Berry, M.S.; Monroe, L. Interpreting enhanced Hg oxidation with Br addition at Plant Miller. *Fuel Process. Technol.*, **2009**, *90*(11), 1372-1377. [http://dx.doi.org/10.1016/j.fuproc.2009.05.022]
- [5] Galbreath, K.C.; Zygarić, C.J. Mercury transformations in coal combustion flue gas. *Fuel Process. Technol.*, **2000**, *65*, 289-310. [http://dx.doi.org/10.1016/S0378-3820(99)00102-2]
- [6] Senior, C.L.; Sarofim, A.F.; Zeng, T.; Helble, J.J.; Mamani-Paco, R. Gas-phase transformations of mercury in coal-fired power plants. *Fuel Process. Technol.*, **2000**, *63*(2), 197-213. [http://dx.doi.org/10.1016/S0378-3820(99)00097-1]
- [7] Eswaran, S.; Stenger, H.G. Effect of halogens on mercury conversion in SCR catalysts. *Fuel Process. Technol.*, **2008**, *89*(11), 1153-1159. [http://dx.doi.org/10.1016/j.fuproc.2008.05.007]
- [8] Zhong, J.; Li, F.; Fan, J. Thermal stability and adsorption of mercury compounds in fly ash. *The Open Fuels & Energy Science Journal.*, **2016**, *9*(1)
- [9] Ghorishi, S.B.; Lee, C.W.; Jozewicz, W.S.; Kilgroe, J.D. Effects of fly ash transition metal content and flue gas HCl/SO<sub>2</sub> ratio on mercury speciation in waste combustion. *Environ. Eng. Sci.*, **2005**, *22*(22), 221-231. [http://dx.doi.org/10.1089/ees.2005.22.221]
- [10] Guo, P.; Guo, X.; Zheng, C.G. Computational insights into interactions between Hg species and  $\alpha$ -FeO (0 0 1). *Fuel*, **2011**, *90*(5), 1840-1846. [http://dx.doi.org/10.1016/j.fuel.2010.11.007]
- [11] Yamaguchi, A.; Akiho, H.; Ito, S. Mercury oxidation by copper oxides in combustion flue gases. *Powder Technol.*, **2008**, *180*(1-2), 222-226. [http://dx.doi.org/10.1016/j.powtec.2007.03.030]
- [12] Presto, A.A.; Granite, E.J. Impact of sulfur oxides on mercury capture by activated carbon. *Environ. Sci. Technol.*, **2008**, *42*(3), 972-973.

- [http://dx.doi.org/10.1021/es7023093] [PMID: 17948811]
- [13] Diamantopoulou, I.; Skodras, G.; Sakellariopoulos, G.P. Sorption of mercury by activated carbon in the presence of flue gas components. *Fuel Process. Technol.*, **2010**, *91*(2), 158-163.  
[http://dx.doi.org/10.1016/j.fuproc.2009.09.005]
- [14] Hughes, K.J.; Ma, L.; Porter, R.T.; Pourkashanian, M. Mercury transformation modelling with bromine addition in coal derived flue gases. *Computer-Aided Chem. Eng.*, **2011**, *29*, 171-175.  
[http://dx.doi.org/10.1016/B978-0-444-53711-9.50035-3]
- [15] Agarwal, H.; Stenger, H.G.; Wu, S.; Fan, Z. Effects of H<sub>2</sub>O, SO<sub>2</sub>, and NO on homogeneous Hg oxidation by Cl<sub>2</sub>. *Energ. Fuel.*, **2006**, *20*
- [16] Ochiai, R.; Uddin, M.A.; Sasaoka, E.; Wu, S. Effects of HCl and SO<sub>2</sub> concentration on mercury removal by activated carbon sorbents in coal-derived flue gas. *Energy Fuels*, **2009**, *23*(10), 52-55.  
[http://dx.doi.org/10.1021/ef900057e]
- [17] Cao, Y.; Gao, Z.; Zhu, J.; Wang, Q.; Huang, Y.; Chiu, C.; Parker, B.; Chu, P.; Pant, W.P. Impacts of halogen additions on mercury oxidation, in a slipstream selective catalyst reduction (SCR), reactor when burning sub-bituminous coal. *Environ. Sci. Technol.*, **2008**, *42*(1), 256-261.  
[http://dx.doi.org/10.1021/es071281e] [PMID: 18350905]
- [18] Cao, Y.; Wang, Q.H.; Li, J.; Cheng, J.C.; Chan, C.C.; Cohron, M.; Pan, W.P. Enhancement of mercury capture by the simultaneous addition of hydrogen bromide (HBr) and fly ashes in a slipstream facility. *Environ. Sci. Technol.*, **2009**, *43*(8), 2812-2817.  
[http://dx.doi.org/10.1021/es803410z] [PMID: 19475955]
- [19] Liu, S.H.; Yan, N.Q.; Liu, Z.R.; Qu, Z.; Wang, H.P.; Chang, S.G.; Miller, C. Using bromine gas to enhance mercury removal from flue gas of coal-fired power plants. *Environ. Sci. Technol.*, **2007**, *41*(4), 1405-1412.  
[http://dx.doi.org/10.1021/es061705p] [PMID: 17593749]
- [20] Hutson, N.D.; Attwood, B.C.; Scheckel, K.G. XAS and XPS characterization of mercury binding on brominated activated carbon. *Environ. Sci. Technol.*, **2007**, *41*(5), 1747-1752.  
[http://dx.doi.org/10.1021/es062121q] [PMID: 17405227]
- [21] Sun, W.; Yan, N.; Jia, J. Removal of elemental mercury in flue gas by brominated activated carbon. *Zhongguo Huanjing Kexue*, **2006**, *26*(3), 257-261.
- [22] Gao, Z.; Ding, Y.; Han, W.; Hu, H.; Lv, S. Species and thermal stability of mercury captured by fly ashes. *Environ. Prog. Sustain.*, **2016**.
- [23] Gao, Z.; Sun, L.; Lv, S.; Yang, P. Research on the effect of additives on mercury speciation in coal fired derived flue gas. *Environ. Prog. Sustain*, **2016**, *35*(6), 1566-1574.  
[http://dx.doi.org/10.1002/ep.12379]
- [24] Standard, A. Standard test method for elemental, oxidized, particle-bound, and total mercury in flue gas generated from coal-fired stationary sources (ontario-hydro). *Designation*, **2008**. D6784-02
- [25] Liu, J.; Cheney, M.A.; Wu, F.; Li, M. Effects of chemical functional groups on elemental mercury adsorption on carbonaceous surfaces. *J. Hazard. Mater.*, **2011**, *186*(1), 108-113.  
[http://dx.doi.org/10.1016/j.jhazmat.2010.10.089] [PMID: 21144653]
- [26] Chen, N.; Yang, R.T. Ab initio molecular orbital calculation on graphite: Selection of molecular system and model chemistry. *Carbon*, **1998**, *36*(7), 1061-1070.  
[http://dx.doi.org/10.1016/S0008-6223(98)00078-5]
- [27] Pople, J.A.; Scott, A.P.; Wong, M.W.; Radom, L. Scaling factors for obtaining fundamental vibrational frequencies and zero point energies from HF/6-31G\* and MP2/6-31G\* harmonic frequencies. *Isr. J. Chem.*, **1993**, *33*(3), 345-350.  
[http://dx.doi.org/10.1002/ijch.199300041]
- [28] Frisch, M.J.; Trucks, G.W.; Schlegel, H.B.; Scuseria, G.E.; Robb, M.A.; Cheeseman, J.R.; Scalmani, G.; Barone, V.; Mennucci, B.; Petersson, G.A. *Gaussian 09W, revision A. 02*; Gaussian Inc: Wallingford, CT, **2009**.
- [29] Gao, Z.; Ding, Y. DFT study of CO<sub>2</sub> and H<sub>2</sub>O co-adsorption on carbon models of coal surface. *J. Mol. Model.*, **2017**, *23*(6), 187.  
[http://dx.doi.org/10.1007/s00894-017-3356-2] [PMID: 28500519]
- [30] Xu, H.; Chu, W.; Huang, X.; Sun, W.; Jiang, C.; Liu, Z. CO<sub>2</sub> adsorption-assisted CH<sub>4</sub> desorption on carbon models of coal surface: A DFT study. *Appl. Surf. Sci.*, **2016**, *375*, 196-206.  
[http://dx.doi.org/10.1016/j.apsusc.2016.01.236]
- [31] Tavakol, H.; Mollaei-Renani, A. DFT, AIM, and NBO study of the interaction of simple and sulfur-doped graphenes with molecular halogens, CH<sub>3</sub>OH, CH<sub>3</sub>SH, H<sub>2</sub>O, and H<sub>2</sub>S. *Struct. Chem.*, **2014**, *25*(6), 1659-1667.  
[http://dx.doi.org/10.1007/s11224-014-0446-y]
- [32] Bader, R.F. A quantum theory of molecular structure and its applications. *Chem. Rev.*, **1991**, *91*(5), 893-928.  
[http://dx.doi.org/10.1021/cr00005a013]
- [33] Lu, T.; Chen, F. Multiwfn: A multifunctional wavefunction analyzer. *J. Comput. Chem.*, **2012**, *33*(5), 580-592.  
[http://dx.doi.org/10.1002/jcc.22885] [PMID: 22162017]
- [34] Humphrey, W.; Dalke, A.; Schulten, K. VMD: Visual molecular dynamics. *J. Mol. Graph.*, **1996**, *14*(1), 33-38, 27-28.

- [http://dx.doi.org/10.1016/0263-7855(96)00018-5] [PMID: 8744570]
- [35] Fujiwara, N.; Fujita, Y.; Tomura, K.; Moritomi, H.; Tuji, T.; Takasu, S.; Niksa, S. Mercury transformations in the exhausts from lab-scale coal flames. *Fuel*, **2002**, *81*(16), 2045-2052.  
[http://dx.doi.org/10.1016/S0016-2361(02)00156-4]
- [36] Lopez-Anton, M.A.; Yuan, Y.; Perry, R.; Maroto-Valer, M.M. Analysis of mercury species present during coal combustion by thermal desorption. *Fuel*, **2010**, *89*(3), 629-634.  
[http://dx.doi.org/10.1016/j.fuel.2009.08.034]
- [37] Rumayor, M.; Diaz-Somoano, M.; Lopez-Anton, M.A.; Martinez-Tarazona, M.R. Mercury compounds characterization by thermal desorption. *Talanta*, **2013**, *114*(3), 318-322.  
[http://dx.doi.org/10.1016/j.talanta.2013.05.059] [PMID: 23953477]
- [38] Sliger, R.N.; Kramlich, J.C.; Marinov, N.M. Towards the development of a chemical kinetic model for the homogeneous oxidation of mercury by chlorine species. *Fuel Process. Technol.*, **2000**, *65-66*(99), 423-438.  
[http://dx.doi.org/10.1016/S0378-3820(99)00108-3]
- [39] Presto, A.A.; Granite, E.J. Survey of catalysts for oxidation of mercury in flue gas. *Environ. Sci. Technol.*, **2006**, *40*(18), 5601-5609.  
[http://dx.doi.org/10.1021/es060504i] [PMID: 17007115]
- [40] Morimoto, T.; Wu, S.; Uddin, M.A.; Sasaoka, E. Characteristics of the mercury vapor removal from coal combustion flue gas by activated carbon using H<sub>2</sub>S. *Fuel*, **2005**, *84*(14-15), 1968-1974.  
[http://dx.doi.org/10.1016/j.fuel.2005.04.007]
- [41] Stolle, R.; Koester, H.; Gutberlet, H. Oxidation and reduction of mercury by SCR DeNOx catalysts under flue gas conditions in coal fired power plants. *Appl. Catal. B*, **2014**, *144*, 486-497.  
[http://dx.doi.org/10.1016/j.apcatb.2013.07.040]
- [42] Niksa, S.; Fujiwara, N. Predicting extents of mercury oxidation in coal-derived flue gases. *J. Air Waste Manag. Assoc.*, **2005**, *55*(7), 930-939.  
[http://dx.doi.org/10.1080/10473289.2005.10464688] [PMID: 16111132]
- [43] Ancora, M.P.; Zhang, L.; Wang, S.; Schreifels, J.; Hao, J. Economic analysis of atmospheric mercury emission control for coal-fired power plants in China. *J. Environ. Sci. (China)*, **2015**, *33*(7), 125-134.  
[http://dx.doi.org/10.1016/j.jes.2015.02.003] [PMID: 26141885]
- [44] Ma, J.J.; Yao, H.; Luo, G.Q.; Fang, X.; Liu, W.; Xu, M.H. Effect of sodium bromide on nitric oxide reduction and mercury oxidation during coal combustion. *J. Eng Thermophys-Rus*, **2010**, *31*(8), 1407-1410.
- [45] Cauch, B.; Silcox, G.D.; Lighty, J.S.; Wendt, J.O.; Fry, A.; Senior, C.L. Confounding effects of aqueous-phase impinger chemistry on apparent oxidation of mercury in flue gases. *Environ. Sci. Technol.*, **2008**, *42*(7), 2594-2599.  
[http://dx.doi.org/10.1021/es702490y] [PMID: 18505002]
- [46] Padak, B. *Mercury reaction chemistry in combustion flue gases from experiments and theory*; Stanford University, **2011**. D
- [47] Padak, B.; Wilcox, J. Understanding mercury binding on activated carbon. *Carbon*, **2009**, *47*(12), 2855-2864.  
[http://dx.doi.org/10.1016/j.carbon.2009.06.029]
- [48] Gale, T.K.; Lani, B.W.; Offen, G.R. Mechanisms governing the fate of mercury in coal-fired power systems. *Fuel Process. Technol.*, **2008**, *89*(2), 139-151.  
[http://dx.doi.org/10.1016/j.fuproc.2007.08.004]
- [49] Senior, C.L. Oxidation of mercury across selective catalytic reduction catalysts in coal-fired power plants. *J. Air Waste Manag. Assoc.*, **2006**, *56*(1), 23-31.  
[http://dx.doi.org/10.1080/10473289.2006.10464437] [PMID: 16499143]
- [50] He, S.; Zhou, J.; Zhu, Y.; Luo, Z.; Ni, M.; Cen, K. Mercury oxidation over a vanadia-based selective catalytic reduction catalyst. *Energy Fuels*, **2008**, *23*(1), 253-259.  
[http://dx.doi.org/10.1021/ef800730f]
- [51] Abad-Valle, P.; Lopez-Anton, M.A.; Diaz-Somoano, M.; Martinez-Tarazona, M.R. The role of unburned carbon concentrates from fly ashes in the oxidation and retention of mercury. *Chem. Eng. J.*, **2011**, *174*(1), 86-92.  
[http://dx.doi.org/10.1016/j.cej.2011.08.053]
- [52] Niksa, S.; Fujiwara, N.; Fujita, Y.; Tomura, K.; Moritomi, H.; Tuji, T.; Takasu, S. A mechanism for mercury oxidation in coal-derived exhausts. *J. Air Waste Manag. Assoc.*, **2002**, *52*(8), 894-901.  
[http://dx.doi.org/10.1080/10473289.2002.10470829] [PMID: 12184687]
- [53] Wilcox, J.; Rupp, E.; Ying, S.C.; Lim, D.; Negreira, A.S.; Kirchofer, A.; Feng, F.; Lee, K. Mercury adsorption and oxidation in coal combustion and gasification processes. *Int. J. Coal Geol.*, **2012**, *90*, 4-20.  
[http://dx.doi.org/10.1016/j.coal.2011.12.003]
- [54] Hower, J.C.; Senior, C.L.; Suuberg, E.M.; Hurt, R.H.; Wilcox, J.L.; Olson, E.S. Mercury capture by native fly ash carbons in coal-fired power plants. *Pror. Energy Combust. Sci.*, **2010**, *36*(4), 510-529.  
[http://dx.doi.org/10.1016/j.pecs.2009.12.003] [PMID: 24223466]
- [55] Huijbregts, W.; Leferink, R. Latest advances in the understanding of acid dewpoint corrosion: Corrosion and stress corrosion cracking in combustion gas condensates. *Anti-Corros. Methods Mater.*, **2004**, *51*(3), 173-188.

- [http://dx.doi.org/10.1108/00035590410533129]
- [56] Persson, K.; Broström, M.; Carlsson, J.; Nordin, A.; Backman, R. High temperature corrosion in a 65 MW waste to energy plant. *Fuel Process. Technol.*, **2007**, *88*(11), 1178-1182.  
[http://dx.doi.org/10.1016/j.fuproc.2007.06.031]
- [57] Zhuang, Y.; Chen, C.; Timpe, R.; Pavlish, J. Investigations on bromine corrosion associated with mercury control technologies in coal flue gas. *Fuel*, **2009**, *88*(9), 1692-1697.  
[http://dx.doi.org/10.1016/j.fuel.2009.01.013]
- [58] Popelier, P.; Bader, R. Effect of twisting a polypeptide on its geometry and electron distribution. *J. Phys. Chem.*, **1994**, *98*(16), 4473-4481.  
[http://dx.doi.org/10.1021/j100067a040]
- [59] Tang, T.; Hu, W.; Yan, D.; Cui, Y. A quantum chemical study on selected  $\pi$ -type hydrogen-bonded systems. *J. Mol. Struct. THEOCHEM*, **1990**, *207*(3-4), 319-326.  
[http://dx.doi.org/10.1016/0166-1280(90)85033-J]
- [60] Carroll, M.T.; Bader, R.F. An analysis of the hydrogen bond in BASE-HF complexes using the theory of atoms in molecules. *Mol. Phys.*, **1988**, *65*(3), 695-722.  
[http://dx.doi.org/10.1080/00268978800101351]
- [61] Carroll, M.T.; Chang, C.; Bader, R.F. Prediction of the structures of hydrogen-bonded complexes using the laplacian of the charge density. *Mol. Phys.*, **1988**, *63*(3), 387-405.  
[http://dx.doi.org/10.1080/00268978800100281]
- [62] Cremer, D.; Kraka, E.; Bader, R.F. Chemical Bonds without Bonding Electron Density—Does the Difference Electron Density Analysis Suffice for a Description of the Chemical Bond? *Angewandte Chemie . International Edition*, **1984**, *23*(8), 627-628.

© 2018 Zhong *et al.*

This is an open access article distributed under the terms of the Creative Commons Attribution 4.0 International Public License (CC-BY 4.0), a copy of which is available at: <https://creativecommons.org/licenses/by/4.0/legalcode>. This license permits unrestricted use, distribution, and reproduction in any medium, provided the original author and source are credited.